

## SUPPORTING INFORMATION FOR

### **Pyranopterin Dithiolene Distortions Relevant to Electron Transfer in Xanthine Oxidase/Dehydrogenase**

Chao Dong, Jing Yang, Silke Leimkühler, and Martin L. Kirk

#### Table of Contents

Substrate Synthesis	2
Enzyme-Product Complex Sample Preparation	2
Spectroscopic Details	3
Computational Details	3
References	4
Cartesian Coordinates	5
Table S1. Selected normal modes	9
Figure S1. Selected normal modes computed for $XO_r$ -4-thioviolapterin	9
Figure S2. Selected normal modes computed for $XO_r$ -2,4-dithioviolapterin	10
Figure S3. Computed HOMO and LUMO for the $XO_{red}$ -4-thioviolapterin complex	11
Figure S4. Electronic absorption spectra for $XO_{red}$ and $XO_{red}$ -P	11
Figure S5. rR overlay of $XO_{ox}$ , $XO_{red}$ , and $XO_{red}$ -2,4-dithioviolapterin	12

## Substrate Synthesis.

**4-thiolumazine:** 4-thiopteridine (4-thiolumazine) was synthesized using a modified method.<sup>(1-3)</sup> The starting material (lumazine; Alfar Aesar ) and Lawesson's (Sigma Aldrich) reagent were obtained commercially and used without further purification. Under an atmosphere of dry nitrogen, a slight excess of Lawesson's reagent (0.51 g, 1.25 mmol) was added to a stirred suspension of lumazine (0.61 g, 2.50 mmol) in dioxane (25 mL) in a three-neck flask at 100 °C. The mixture was refluxed at this temperature for 15 minutes during which time the solution color changed from pale yellow to dark red. The reaction was monitored by thin layer chromatography. Upon completion, the reaction mixture was cooled to room temperature and evaporated to dryness in a vacuum. The crude product was washed with acetic acid followed by water. After drying in vacuo, the reaction yielded 300 mg (75%) of dark red powder. Crystals for x-ray diffraction were obtained by slow evaporation of saturated 4-thiolumazine dimethylformamide solution. The ESI-MS (HCOOH):  $m/z$  *calc* =180,  $m/z$  *exp* = 181.02 (M+H). <sup>1</sup>H NMR ( $\delta$ , ppm): 13.94 (s), 13.68 (s), 8.73 (d), 8.59(d). <sup>13</sup>C NMR ( $\delta$ , ppm): 191.00, 148.55, 147.67, 146.47, 141.07, 130.98.

**2,4-dithiolumazine:** The starting material, 2-thiolumazine, was prepared as previously described.<sup>(2)</sup> Under an atmosphere of dry nitrogen, a slight excess of Lawesson's reagent (0.51 g, 1.25 mmol) was added into a stirred suspension of 2-thiolumazine (0.45 g, 2.50 mmol) in dioxane (25 mL) in a three-neck flask at 100 °C. The mixture was refluxed for 15 minutes during which time the solution color changed from pale yellow to dark red. Upon completion, the reaction mixture was cooled to room temperature and evaporated to dryness in a vacuum. The crude product was washed with acetic acid followed by water. After drying in vacuo, the reaction yielded 245 mg (50%) of orange powder. The ESI-MS (HCOOH):  $m/z$  *calc* =196,  $m/z$  *exp* = 196.99 (M+H). <sup>1</sup>H NMR ( $\delta$ , ppm): 13.08 (s), 13.27 (s), 8.66 (d), 8.55(d). <sup>13</sup>C NMR ( $\delta$ , ppm): 187.73, 172.75, 149.27, 144.73, 142.56, 133.49.

## Enzyme-Product Complex Sample Preparation.

Oxidized *B. taurus* XO was purchased from Sigma Aldrich. The XO<sub>red</sub>-product complex can be prepared in one of two methods. In the first method, the enzyme-product complex was produced by reacting oxidized xanthine oxidase with the substrate (4-thiolumazine or 2,4-dithiolumazine), followed by dithionite reduction. The formation of XO<sub>red</sub>-4-thioviolapterin was initiated by adding 15  $\mu$ L 7.8 mM 4-thiolumazine to a solution containing 70  $\mu$ L 72  $\mu$ M XO<sub>ox</sub> and 60  $\mu$ L 50mM sodium bicine-NaOH (pH=8.3) buffer. The solution mixture was incubated for 5 minutes at room temperature under aerobic conditions, and then bubbled with nitrogen gas for 15 minutes to make anaerobic. The reaction mixture was titrated with 15  $\mu$ L 0.4 M sodium dithionite in an anaerobic environment. Spectrophotometric measurements have established the

formation of  $\text{XO}_{\text{red}}$ -4-thioviolapterin complex through the appearance of an absorbance maximum in the electronic absorption spectrum at 758 nm.

A second method may also be used to generate the enzyme-product complex. Here, 15  $\mu\text{L}$  7.8 mM of 4-thiolumazine was added to 70  $\mu\text{L}$  of 72  $\mu\text{M}$   $\text{XO}_{\text{ox}}$  and buffer solution for 2 hours. This mixture was then separated using an Amicon Ultra 0.5mL centrifugal filter (Sigma-Aldrich: MWCO 3kDa). The separated product solution was then quickly added to a fresh, anaerobic, dithionite reduced XO sample (15  $\mu\text{L}$  0.4 M), after which the electronic absorption spectrum was measured. The appearance of the 758 nm band confirmed the presence of the enzyme-product complex.

Wild-type *R. capsulatus* XDH was expressed in *E. coli* as previously described.<sup>(4)</sup> The  $\text{XDH}_{\text{red}}$ -product complexes were generated using the same methods that were used for XO.

## **Spectroscopic Details.**

### Electronic Absorption Spectroscopy.

Electronic absorption spectra were collected using a double-beam Hitachi U-4100 UV-vis-NIR spectrophotometer (Hitachi High-Technologic Corporation) capable of scanning a wavelength range between 185 and 3200 nm. Absorption spectra were measured in a 1 cm path length, black-masked, quartz cuvette (Starna Cells, Inc.) equipped with a Teflon stopper. The instrument was calibrated with reference to the 656.10 nm deuterium line.

### Resonance Raman Spectroscopy.

Solution resonance Raman spectra (rR) were collected on a DXR Smart Raman Instrument (Thermo Fisher Scientific Inc.). All aqueous samples were sealed in capillary tubes with a diameter of 1.5 - 1.8 mm and mounted onto the capillary tube holder in a 180° back scattering accessory chamber. A 780 nm diode laser was used as the excitation source and the excitation power was 140 mW. A buffer background and a standard sample ( $\text{Na}_2\text{SO}_4$ ) were collected before the data collection. Raman shifts were calibrated against the standard sulfate peak at 992  $\text{cm}^{-1}$ . A buffer background spectrum was subtracted from the raw data to yield the final Raman spectrum.

## **Computational Details.**

Spin-restricted gas phase geometry optimizations, numerical frequency calculations, and excited states computations for the  $\text{XO}_{\text{red}}$ -product complexes were performed at the density functional theory (DFT; TDDFT) level using the Gaussian

03W<sup>(5)</sup> and ORCA (version 2.9.1) software packages.<sup>(6)</sup> All Gaussian 03W calculations used the B3LYP hybrid exchange-correlation functional. A 6-31g\* basis set was used for all atoms except for molybdenum where a LANL2DZ basis set, which included an effective core potential, was used. The vibrational frequencies were then calculated based on this optimized geometry. All of these computations employed the BP86 functional with the def2-TZVP basis set for Mo and S, and def2-SVP for all light atoms. The vibrational modes were visualized and rendered using ChemCraft(version 1.7).

## References:

1. Gorizdra, T.E. Khimiya Geterotsiklieheskikh Soedinenii, 1969, 5, 908-912.
2. Schneider, H. J.; Pfeleiderer, W. Chem. Ber, 1974, 107, 3377.
3. Felczak, K.; Bretner, M.; Kulikowski, T.; Shugar, D. Nucleosides & nucleotides. 1993, 12, 245-261.
4. Truglio, J. J.; Theis, K.; Leimkühler, S.; Rappa, R.; Rajagopalan, K.V.; Kisker, C., *Structure*. 2002, 10, 115-125.
- 5 Gaussian 09, Revision C.1, M. J. Frisch, G. W. Trucks, H. B. Schlegel, G. E. Scuseria, M. A. Robb, J. R. Cheeseman, G. Scalmani, V. Barone, B. Mennucci, G. A. Petersson, H. Nakatsuji, M. Caricato, X. Li, H. P. Hratchian, A. F. Izmaylov, J. Bloino, G. Zheng, J. L. Sonnenberg, M. Hada, M. Ehara, K. Toyota, R. Fukuda, J. Hasegawa, M. Ishida, T. Nakajima, Y. Honda, O. Kitao, H. Nakai, T. Vreven, J. A. Montgomery, Jr., J. E. Peralta, F. Ogliaro, M. Bearpark, J. J. Heyd, E. Brothers, K. N. Kudin, V. N. Staroverov, R. Kobayashi, J. Normand, K. Raghavachari, A. Rendell, J. C. Burant, S. S. Iyengar, J. Tomasi, M. Cossi, N. Rega, J. M. Millam, M. Klene, J. E. Knox, J. B. Cross, V. Bakken, C. Adamo, J. Jaramillo, R. Gomperts, R. E. Stratmann, O. Yazyev, A. J. Austin, R. Cammi, C. Pomelli, J. W. Ochterski, R. L. Martin, K. Morokuma, V. G. Zakrzewski, G. A. Voth, P. Salvador, J. J. Dannenberg, S. Dapprich, A. D. Daniels, Ö. Farkas, J. B. Foresman, J. V. Ortiz, J. Cioslowski, and D.J. Fox, Gaussian, Inc., Wallingford CT, 2009.
6. Neese, F. ORCA, an ab initio, density functional, and semiempirical program package; University of Bonn: Bonn, Germany,

**Cartesian coordinates for the optimized XOr-(4-thioviolapterin) structure:**

N	7.055834	0.281855	1.287625
C	8.259531	-0.371689	1.081407
N	8.198207	-1.305489	0.058589
C	7.100939	-1.654001	-0.765820
C	5.893706	-0.923607	-0.487187
C	3.678591	-0.416705	-0.871867
N	4.734008	-1.133015	-1.196093
C	3.669136	0.582239	0.189169
C	5.876129	0.062781	0.560693
N	4.829289	0.794801	0.902911
C	-2.552087	-1.681857	2.876692
C	-2.317921	-1.772878	1.378625
O	-3.644552	-2.032795	0.847618
C	-1.613122	-0.606678	0.709635
S	0.072596	-0.285544	1.193284
C	-2.191879	0.100302	-0.305754
S	-1.355069	1.427265	-1.142773
N	-7.455201	-1.858275	-0.654157
C	-8.467573	-1.052155	-0.444648
N	-9.795138	-1.527578	-0.505449
N	-8.298151	0.289834	-0.212218
C	-7.034119	0.945724	-0.149932
O	-6.974677	2.162711	0.083866
N	-4.636575	0.506021	-0.344872
C	-3.535916	-0.299469	-0.869646

C	-3.799821	-1.787535	-0.542156
N	-5.135651	-2.168943	-0.932529
C	-5.928105	0.044871	-0.395703
C	-6.197379	-1.311801	-0.651782
O	2.620298	1.253166	0.498894
O	0.364769	3.107669	1.107959
Mo	0.695561	1.788383	0.087262
S	1.577524	2.505730	-2.054984
C	-2.081360	-0.755410	3.727179
H	-1.416076	0.051819	3.378853
H	-2.329089	-0.804452	4.801380
H	-3.201364	-2.498276	3.248085
H	-4.481635	1.503776	-0.190404
H	-5.369969	-3.158479	-0.820399
H	-9.102734	0.916681	-0.127525
H	-9.759322	-2.547329	-0.615921
H	-10.333404	-1.303433	0.342660
H	7.018833	0.988428	2.026171
H	9.058972	-1.822384	-0.138516
H	2.920006	2.504403	-1.752367
H	2.743110	-0.566224	-1.441713
H	-3.070785	-2.400936	-1.127878
H	-3.477094	-0.204993	-1.984394
H	-1.688548	-2.690507	1.201533
S	7.363190	-2.850233	-1.930093
O	9.280082	-0.146188	1.739867

**Cartesian coordinates for the optimized XOr-(2,4-thioviolapterin) structure:**

N	6.804920	0.193794	1.060285
C	7.948378	-0.517544	0.811601
N	7.821387	-1.445127	-0.185429
C	6.680722	-1.751573	-0.973856
C	5.519886	-0.963207	-0.659379
C	3.320453	-0.353836	-0.966596
N	4.328661	-1.121879	-1.325526
C	3.395967	0.648506	0.087118
C	5.585577	0.029063	0.379834
N	4.590872	0.812399	0.756772
C	-2.697394	-1.599403	2.915962
C	-2.472465	-1.698791	1.417126
O	-3.794707	-1.996930	0.897088
C	-1.802537	-0.520526	0.733600
S	-0.119326	-0.161209	1.194867
C	-2.407927	0.167690	-0.278783
S	-1.607519	1.505602	-1.133905
N	-7.618949	-1.934733	-0.585441
C	-8.651741	-1.156260	-0.371257
N	-9.965511	-1.668040	-0.428605
N	-8.518185	0.189598	-0.138474
C	-7.271978	0.879665	-0.083127
O	-7.244290	2.097819	0.150589
N	-4.864114	0.506194	-0.289762
C	-3.747481	-0.268031	-0.826902

C	-3.966344	-1.762422	-0.492954
N	-5.293284	-2.182060	-0.872591
C	-6.143388	0.009584	-0.334789
C	-6.376463	-1.354077	-0.588306
O	2.390162	1.368390	0.429955
O	0.142382	3.234719	1.065115
Mo	0.459308	1.904299	0.054605
S	1.294577	2.594704	-2.116030
C	-2.248092	-0.649889	3.752458
H	-1.610623	0.173550	3.390627
H	-2.485205	-0.694258	4.829158
H	-3.318616	-2.430795	3.301575
H	-4.738383	1.508970	-0.141782
H	-5.499107	-3.177928	-0.761304
H	-9.339381	0.793957	-0.050006
H	-9.903226	-2.687142	-0.533448
H	-10.510972	-1.452319	0.417031
H	6.835793	0.903115	1.797034
H	8.652757	-2.001104	-0.404128
H	2.640399	2.617789	-1.832003
H	2.359155	-0.461883	-1.501439
H	-3.224529	-2.357268	-1.081496
H	-3.703899	-0.175066	-1.942452
H	-1.819941	-2.600525	1.243307
S	6.855920	-2.965986	-2.132638
S	9.386747	-0.268972	1.662131



**Table S1. Selected normal modes for XOr-4-thioviolapterin and XOr-2,4-dithioviolapterin**

XOr-4-thioviolapterin		Mode Description	XOr-2,4-dithioviolapterin		Mode Description
Exp Freq (cm <sup>-1</sup> )	Cal Freq (cm <sup>-1</sup> )		Exp Freq (cm <sup>-1</sup> )	Cal Freq (cm <sup>-1</sup> )	
234	234	Fig. S1A	234	242	Fig. S2A
259	259	Fig. S1B	259	262	Fig. S2B
290	287	Fig. S1C	283	290	Fig. S2C
328	333	Fig. S1D	326	334	Fig. S2D
352	352	Fig. S1E	352	351	Fig. S2E
408	409	Fig. S1F			
			411	423	Fig. S2G
			440	442	Fig. S2H
493	487	Fig. S1I	513	501	Fig. S2I

**Figures. Selected Computed Normal Modes**

Figure S1. Selected normal modes computed for XOr<sub>r</sub>-4-thioviolapterin.

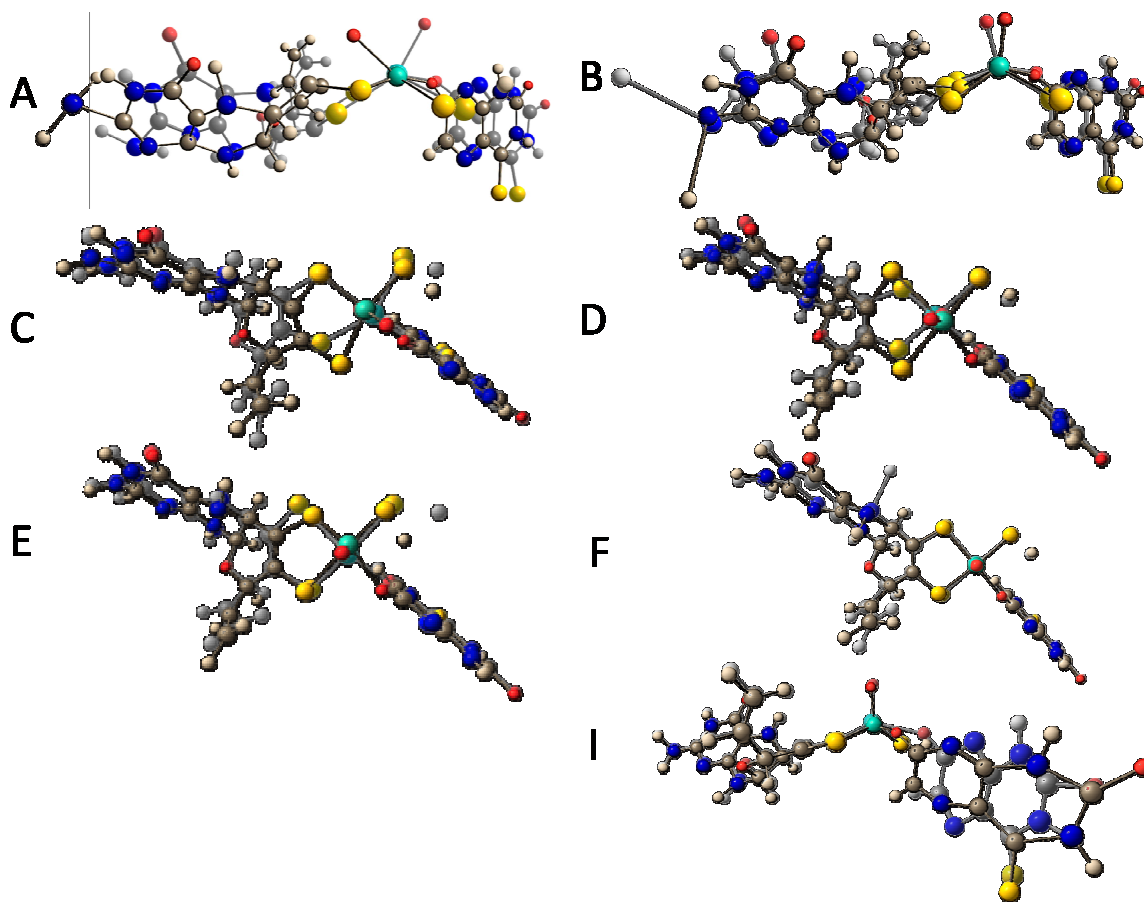


Figure S2. Selected normal modes computed for XO<sub>r</sub>-2,4-dithioviolapterin.

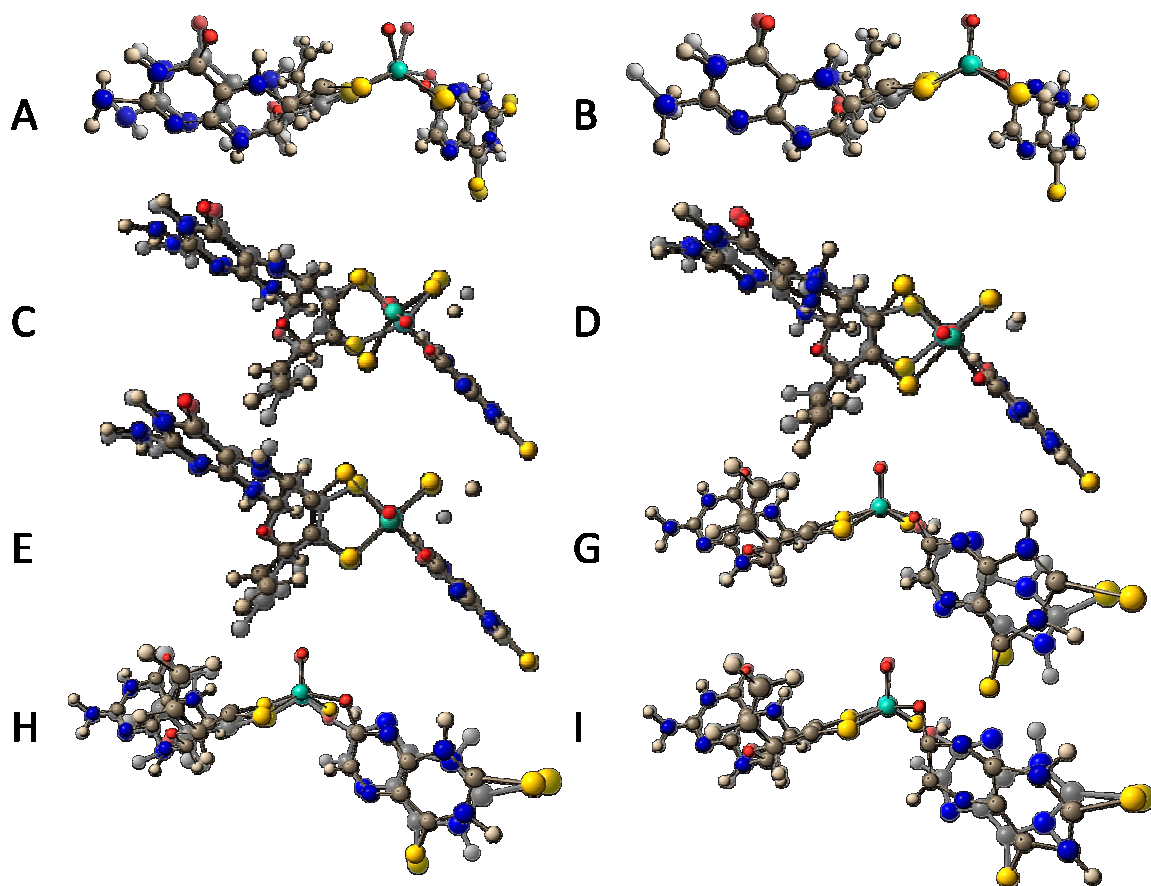


Figure S3. Computed HOMO and LUMO for the  $XO_{red}$ -4-thioviolapterin complex. The MLCT band derives from a HOMO to LUMO one-electron promotion. Here, the HOMO possess ~69% Mo dxy character and only ~12% of product ring  $\pi$  character. In marked contrast, the LUMO possesses only ~6% Mo dxy character and ~83% product ring character.

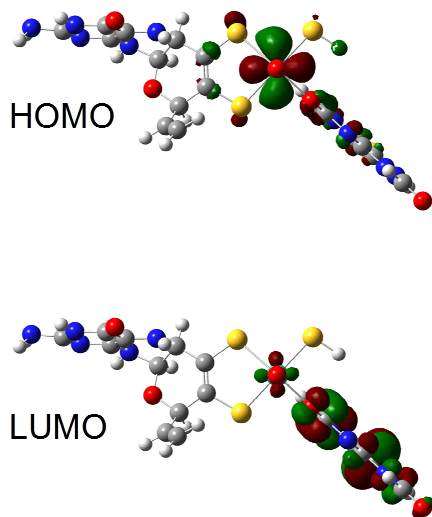


Figure S4. Electronic absorption spectra for  $XO_{red}$  and  $XO_{red}$ -P

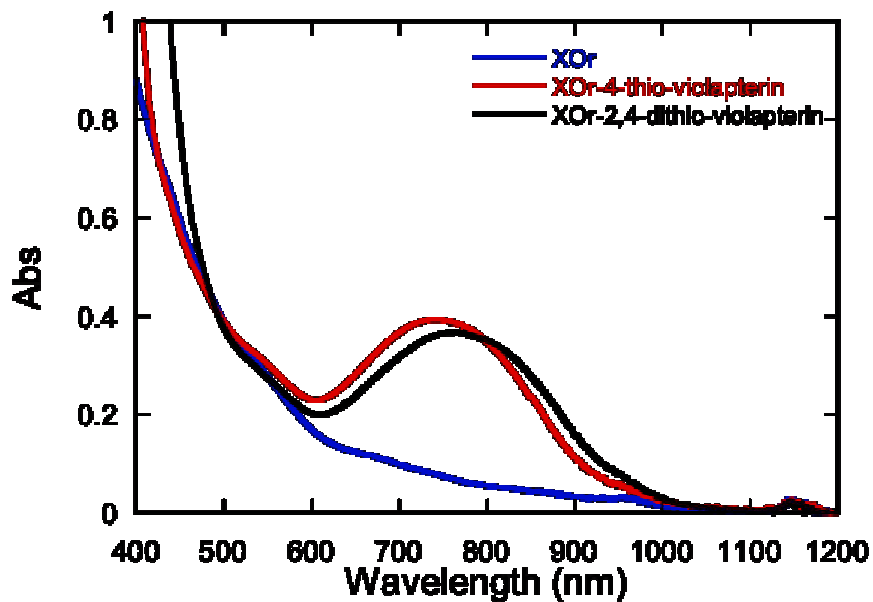


Figure S5. Resonance Raman overlay of  $XO_{ox}$ ,  $XO_{red}$ , and the  $XO_{red}$ -2,4-dithioviolapterin complex (72  $\mu M$ ). The asterisk is the  $(NH_4)_2SO_4$  peak from the commercial XO buffer, and the spectra are normalized to this peak.

